

**Water balance modeling in Mediterranean water limited ecosystem using vegetation parameters and soil moisture from remote sensing**

Detto M., Mancini M., Martinelli J., Montaldo N.

in

Hamdy A. (ed.), Monti R. (ed.).  
Food security under water scarcity in the Middle East: Problems and solutions

Bari : CIHEAM  
Options Méditerranéennes : Série A. Séminaires Méditerranéens; n. 65

2005  
pages 225-236

Article available on line / Article disponible en ligne à l'adresse :

<http://om.ciheam.org/article.php?IDPDF=5002217>

To cite this article / Pour citer cet article

Detto M., Mancini M., Martinelli J., Montaldo N. **Water balance modeling in Mediterranean water limited ecosystem using vegetation parameters and soil moisture from remote sensing.** In : Hamdy A. (ed.), Monti R. (ed.). *Food security under water scarcity in the Middle East: Problems and solutions.* Bari : CIHEAM, 2005. p. 225-236 (Options Méditerranéennes : Série A. Séminaires Méditerranéens; n. 65)



<http://www.ciheam.org/>  
<http://om.ciheam.org/>

# WATER BALANCE MODELING IN MEDITERRANEAN WATER LIMITED ECOSYSTEM USING VEGETATION PARAMETERS AND SOIL MOISTURE FROM REMOTE SENSING

M. Detto, M. Mancini\*, J. Martinelli, N. Montaldo

\* DIIAR Politecnico di Milano, Milano, Italy. E-mail: [marco.mancini@polimi.it](mailto:marco.mancini@polimi.it)

**SUMMARY** – The assimilation of remote sensing data in hydrologic models allows improving water and energy balance predictions as assessed in several literature articles in the last decade due to the similar pixel size at which digital information from remote sensing and distributed water balance modeling refers. In this paper we present an application of the combined use of remote information and hydrological modeling on a monitored basin in the Italian semi arid area, using the remote sensing analysis for hydrological model parameterization and model validation. In fact we retrieve at pixel scale vegetation parameter as the leaf area index (LAI) used in the computation of evapotranspiration and surface soil moisture images used as “internal” control variable of model behavior. The LAI is obtained from Quikbird satellite using visible and near infrared images while the soil moisture is retrieved from microwave ASAR (Advanced Synthetic Aperture Radar on the European Space Agency satellite Envisat). Discussion of result is then provided in term of data reliability with perspective of operative use as aid the in the irrigation practice and in a real time monitoring of fluxes between land surfaces and the atmosphere boundary layer.

**Keywords:** Water balance, hydrological modeling, remote sensing, soil moisture

## 1. INTRODUCTION

The agricultural development in semi-arid regions, such as Italy's southern region and islands, suffers from water scarcity. These impacts are associated with broad desertification processes of the Mediterranean area (e.g., Piervitali *et al.* 1999; Showstack, 2001) and increased pressures on water supplies by civil and industrial utilizations.

Achieving a rational and efficient use of water and other agro-forest resources through employment of modern information systems (D'Urso and Santini, 2001) is a primary objective in these area for the promotion of a “sustainable development” politic.

Evapotraspiration, the combined flux of plant transpiration and evaporation fro soil, also known as the latent heat, strongly influence the soil water balance especially in semi arid regions. In fact transpiration fluxes exerted from the vegetation are still observable from surface dry soil due to the plants and routs dynamic. The interaction between soil moisture and vegetation dynamic, especially due to the strong non-linearity that characterize their relationship (Rodriguez-Iturbe, 2000), can present one of the main contribution in improving the real water demand for an agricultural district and the practice of irrigation trying to achieve a more efficient water use.

Now days the development of “gis” based water balance models and the satellite sensors for land observation and monitoring can be a formidable tool for improve results in term of more accurate simulations and irrigation efficiency. The synergic approach of satellite data and distributed water balance parametrization is intuitive because both tools refer to the pixel scale, but at same time the quantitative use of this still need an improvement from researchers and techniques.

Among variables and parameters the presented paper focus on the surface soil moisture variable and leaf area index parameter and how both can be estimated from comparison of satellite data and ground measurement.

Soil moisture content is widely known to be the key state variable of the soil-vegetation-lower atmosphere system for its leading role in surface water and energy balances (e. g., Famiglietti and

Wood, 1994; Wigmosta *et al.*, 1994), from the meso, small basin to the field scale. High resolution Satellite radar images offers the opportunity for monitoring surface soil moisture at high spatial resolution (up to 15 m), which is suitable for distributed mapping at the small scales of typical Mediterranean basins. In the last two decades researchers attracted from this potentiality have shown performances and limits of this technology (Fung, 1992, Jackson, 1996, Mancini, 1999). In this paper we use the ASAR sensor high resolution images for estimating surface soil moisture via an inversion technique based on the Integral Equation Model of Fung *et al.* (1992). The obtained values are compared with ground measurement and water balance modeling results.

Leaf area index is one of the variables that characterize the vegetation type and its stage, and according to the Monteith researches define the evapotranspiration fluxes using the well assessed Penman evaporation equations. The possibility to obtain robust empirical models for deriving LAI from visible and infrared spectral channels of remote sensing images in the Mulargia basin is investigated. Using several available satellite. In the paper only result from the Quickbird images (spatial resolution of 2.8 m) of May 2004 are discussed.

## 2. THE CASE STUDY AREA

The Mulargia river basin (area of about 65 km<sup>2</sup>, Figure 1) is a sub-basin of the Flumendosa river, located in center-east Sardinia. The basin has a key role in the water resources management of Sardinia and is an experimental basin of Politecnico di Milano since 2003.

Mean annual rainfall for the basin is about 690 mm. The rainiest months are December and January, and the driest month is July. The soils in the basin are generally of modest thickness (< 1-2 m), and the microrelief frequently rocky. The vegetation throughout the basin has been in part altered by human activities, with many areas (before covered by scrubs) converted to pasture. Urbanized areas are a minor component (about 2.5 %). Agricultural activities (other than the open pasture mentioned above) are also relatively minor, so that the use of water for irrigation is negligible.

The area's topography is available in a digital format through the DEM at 30 m spatial resolution (Figure 2). Geolithologic, land use and pedologic information of the Mulargia basin are also available.

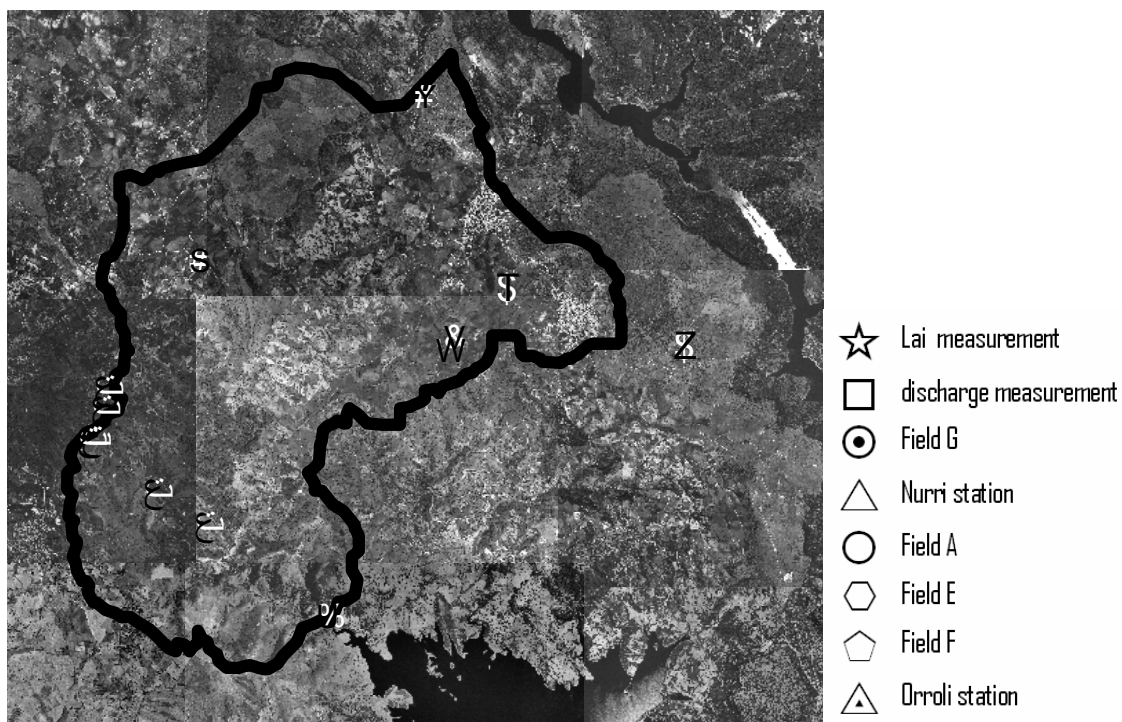


Figure 1. Aerial photography of the Mulargia basin; symbols are listed in the legend.

Rainfall, air temperature data and discharge measurements (from Authority of water district: Ente Autonomo del Flumendosa), relatively to the basin outlet section, are available at hourly time resolution. Historical hydrologic data series of the Nurri station are also available for the period 1922-1992.

From April 2003 data of evapotranspiration, net radiation, latent and sensible heat flux, soil moisture, surface temperature, air humidity and temperature, rain and wind velocity are measured by a micrometeorological eddy-correlation (e.g., Brutsaert, 1982) tower (Figura 1). During the same period field campaigns were performed all over the basin measuring LAI and soil moisture (figure 1).

Table 1. Timetable of the soil moisture field campaigns during 2003, computed by TDR (T) and gravimetric (G) measurements in several fields of the study area

Field	Date																
	14/3	26/3	8/4	14/4	24/4	30/4	13/5	19/5	29/5	4/6	17/6	23/6	13/8	18/9	6/10	6/11	15/12
A	T-G	T-G	T	T-G	T	T	T-G	T	T-G	G	G	G	G	T	T-G	T-G	T-G
B	T-G	T-G	T	T-G													
C	T-G	T-G	T	T-G													
D	T-G	T-G	T	T-G													
E		T-G	T	T-G	T	T	T-G	T	G	G	G	G	G	T	T-G	T-G	T-G
F		T-G	T	T-G	T	T	G	T	G		G	G	G	T	T-G	T-G	T-G
G			T	T-G	T	T	G	T	G	G	G	G	G	T	T-G	T-G	T
I				G	T		T-G		G	G	G	G	G	T	T-G	T-G	T-G

### 3. SOIL MOISTURE FROM SATELLITE DATA

The retrieve of superficial soil moisture from remote sensing is very attractive from the hydrologic point of view due to the possibility to map the values at detailed pixel scale and the well known crucial role that this variable play on the fluxes rate and then on the overall water balance. For this reason several papers have pointed out performance and limit of different techniques from different sensor type. In this paper according to the most assessed literature on the argument we present an application of radar signal inversion for assessing soil moisture

For shortness of space here after we mention the used procedure giving directly the results of the inversion techniques in terms of soil moisture.

High resolution data of the new ASAR (Advanced Synthetic Aperture Radar) sensor aboard European Space Agency's Envisat satellite offers the opportunity for monitoring surface soil moisture at high spatial resolution, 30 m, with multitemporal, multipolarization, and multiple incidence angle images. The physical link between the radar signal,  $\sigma^0$ , and soil water content is given by the dependency of radar signal not only from the surface roughness but also from the dielectric constant of the soil (Figure 2).

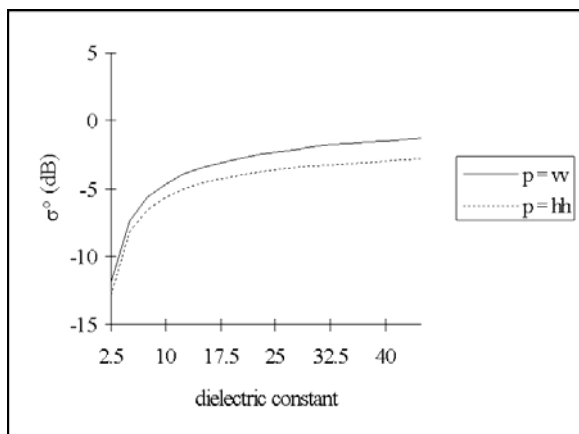


Figure 2. The relation between backscattering signal and dielectric constant for vertical , vv, and horizontal , hh, polarization.

Dielectric constant is a function of the soil moisture ,  $\theta$ , and can be modelled using the Topp equation (Topp et.al 1980)

$$\theta = (-530 + 292 \varepsilon - 5.5\varepsilon^2 + 0.043\varepsilon^3) \cdot 10^{-4} \quad (1)$$

The retrieving of the dielectric constant and then soil moisture from an operative radar images may be obtained from empirical as well physically based electromagnetic models. We have always preferred the use of the second type because a physically based model is site independent and this allows to increase the multitemporal frequency ( up to three days from 30 days in the operative satellite phase) using images belonging to data take that have not necessarily the same reading geometry. This peculiarity is essential for the soil moisture monitoring for which the temporal variability is much less than the 30 days repeat cycle ( Altese *et al.*, 1996, Mancini *et al.*, 1999, Quesney *et al.*, 2000)

For a proper interpretation of the radar signal in this heterogeneous basin, first the effect of the vegetation is considered through the model of Quesney *et al.* (2000), which allows to the observed backscattering coefficient is the sum of a bare soil component and a vegetation component, which is function of the leaf size and the vegetation height.

Then, for deriving the soil moisture from the radar signal ( $\sigma^\circ$ ) the Integral Equation Model (IEM) of Fung *et al.* (1992) and the Topp *et al.* (1980) model are used. Indeed, the IEM estimates the dielectric constant ( $\varepsilon$ ) from  $\sigma^\circ$  using:

$$\sigma^\circ = \sigma^\circ(\dots\varepsilon, \sigma, L) \quad (2)$$

where  $\sigma$  is the standard deviation and  $L$  is the autocorrelation length of the surface micro roughness. For solving (1) and estimating  $\varepsilon$  the  $\sigma$  e  $L$  parameters need to be determined trough field estimates of  $\varepsilon$ , which can be made locally using, for instance, TDR measurements of the dielectric constant. But then one of two parameters needs to be determined for solving (2). In this sense, the new ASAR sensor provide double information because the images are double polarization so that the system of the two IEM equations can be solved for  $\sigma$  e  $L$  (known the  $\varepsilon$  value measured locally on the field):

$$\begin{cases} \sigma_{VV}^\circ = \sigma^\circ(\dots\varepsilon, \sigma, L) \\ \sigma_{HH}^\circ = \sigma^\circ(\dots\varepsilon, \sigma, L) \end{cases} \quad (3)$$

After the local calibration of  $\sigma$  e  $L$ , basin maps of  $\varepsilon$  are derived, which basin and field spatial average are compared with model and ground measurements of soil moisture in following.

#### 4. VEGETATION PARAMETERES FROM SATELLITE DATA

The observation of the Earth in the VIS and NIR regions of the electromagnetic spectrum by passive remote sensors have been used in the last three decades to monitor land surface and obtain important parameters especially in the case of vegetation cover, i.e. fraction of cover, vegetation index (VI), albedo, type classification and leaf area index (LAI) defined as single-side leaf area per unit ground area.

In particular, for the latter, several studies have proved his dependence on the measurements of reflectance in the red (R) and infrared (IR) bands (e.g., Chen and Cihlar, 1996, Carlson and Ripley, 1997, Green *et al.*, 1997, Gupta *et al.*, 2000) that can be combined in different vegetation indexes, the most common is called NDVI defined as:

$$NDVI = (IR - R)/(IR + R) \quad (4)$$

A simple approach is based on empirical relationships calibrated upon limited ground-based measurements of LAI connected to the satellite passages. Since the relation between LAI-NDVI

suffers of a marked decrease in sensibility as the LAI increases due to a saturation of the remotely sensed signal, non linear functions are required to match the observations.

The LAI measurements, as the retrieved NDVI, are intended spatially-averaged on a homogeneous vegetation pattern that contains within the image a consistent number of pixel.

Limitations to this methodology have be found in many factors, such as leaf optical properties of the different species, orientation of the surface with respect to the illumination and viewing angle (in the case of topography), background effects of under-story and bare soil reflectance and errors in LAI measurements particularly when not destructive methods are adopted.

An important point is represented by the spatial resolution of the satellite image that must be enough fine to not include heterogeneity effect within each pixel related to the degree of heterogeneity of the studied area (Chen, 1999, Friedl *et al.*, 1995). A wild range of spatial resolutions are available and in this direction new satellites are permitting unprecedented high mapping (~1-10 m<sup>2</sup>) of the landscape (albeit at low spectral resolution). Consequently a resize of the map is required by the, usually coarser, distributed hydrological model grid, resize that takes into account the variability of the land cover especially in Mediterranean ecosystems where the patchiness of the vegetation distribution is on the order of several square meters.

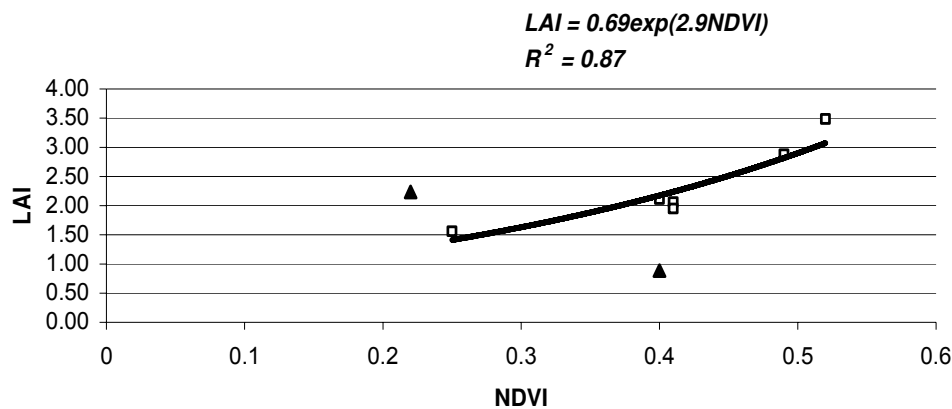


Figure 3. Regression between LAI measurements and NDVI from QuickBird image; triangle dots are excluded from the regression.

In this work not destructive LAI measurements were made using an optical instrument: LAI-2000, Li-COR (Welles and Norman, 1991), on different vegetation cover types and related to NDVI retrieved from QuickBird images (spat. res. 2.8m x 2.8m) acquired in May 2004. As shown in Figure 2, an exponential relationship is found to best match the observations (coefficient of determination equal to 0.87) excluding two points that show singularity behavior. One of them was a field of sparse Eucalyptus trees where the presence of grass under-story increased the value of NDVI, the other one were located in a slope terrain that could produce an underestimation of NDVI. By this relationship a map of LAI was obtained and resized to a coarser grid (100m x 100m) using a nearest neighbor resampling (Richards, 1999) (Figure 4).

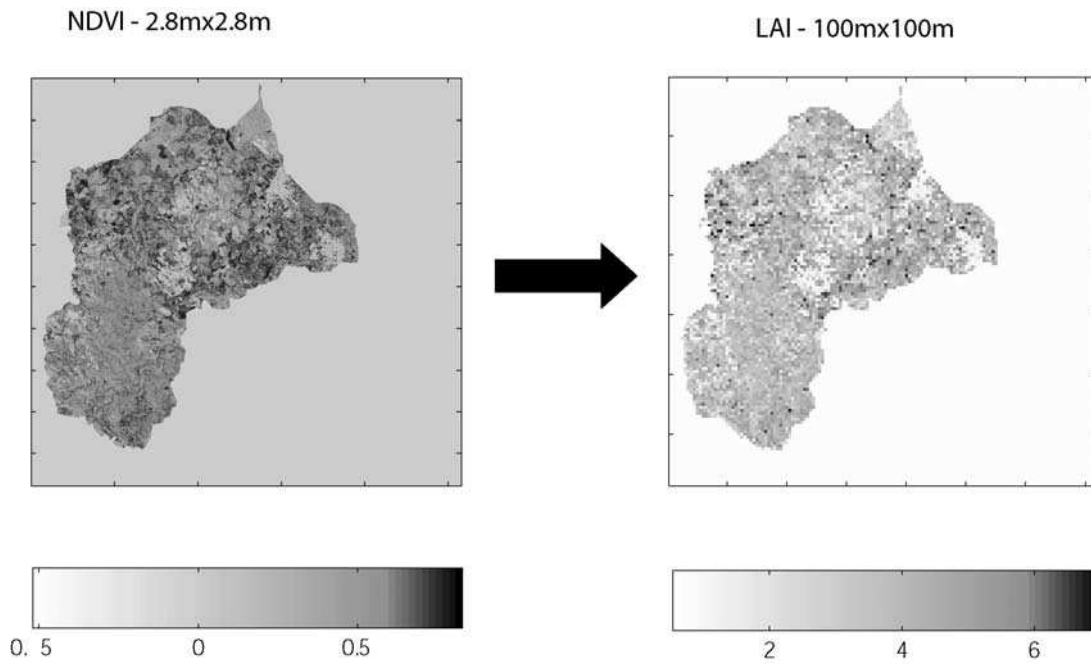


Figure 4. NDVI map from QuickBird image (spat. res. 2.8m x 2.8m) on the left. Evaluated LAI map (spat. res. 100m x 100m) on the right.

In Figure 5 the frequency of LAI distribution is plotted for different size resampling showing that the statistic is preserved passing from the finer 2.8 m resolution to a coarser grid (100 m pixel size) used in the water balance model, even if a little decrease in the peak is observed.

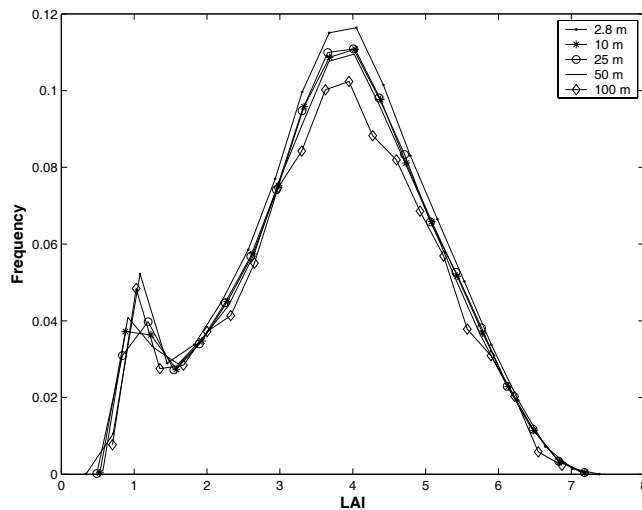


Figure 5. Frequency of LAI distribution for different size resampling

## 5. HYDROLOGICAL WATER BALANCE MODEL

The basic force-restore equations for the prediction of the land surface fluxes and the evolution of surface temperature and moisture content are well described elsewhere (Noilhan and Planton, 1989; Noilhan and Mahfouf, 1996, Montaldo and Albertson, 2001). For context we review the soil moisture evolution equations here. The model considers near surface and deep (root zone) soil layers of depths  $d_1$  and  $d_2$  and volumetric water contents  $\theta_g$  and  $\theta_2$ , respectively as shown (Figure 6).

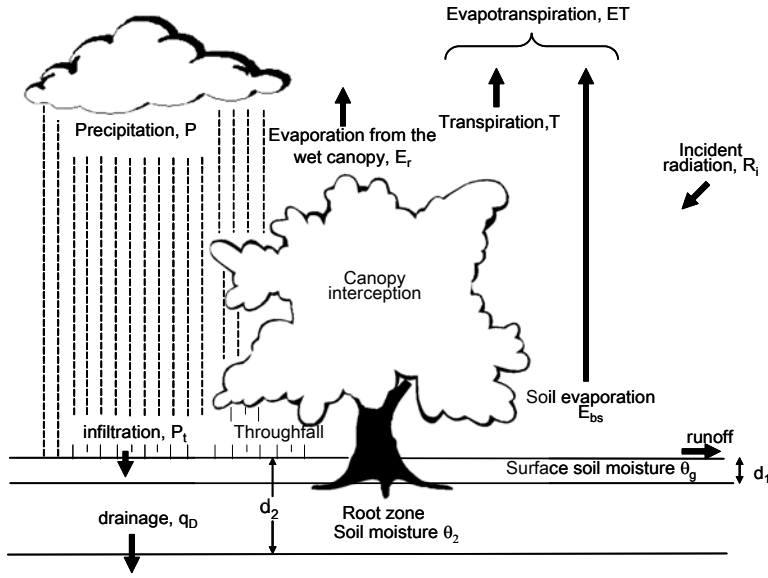


Figure 6. Schematic representation of the bucket model

The soil moisture in the two layers, that represent the state variables of the model evolve according to:

$$\frac{\partial \theta_g}{\partial t} = \frac{C_1}{\rho_w d_1} (P_g - E_g) - \frac{C_2}{\tau} (\theta_g - \theta_{geq}) \quad 0 \leq \theta_g \leq \theta_s \quad (5)$$

$$\frac{\partial \theta_2}{\partial t} = \frac{1}{\rho_w d_2} (P_g - E_g - E_{tr} - q_2) \quad 0 \leq \theta_2 \leq \theta_s \quad (6)$$

where  $P_g$  is the precipitation rate infiltrating into the soil calculated with the Philip's infiltration model (Philip, 1960),  $E_g$  the bare soil evaporation rate,  $E_{tr}$  the transpiration rate from the root zone ( $d_2$ ),  $q_2$  the rate of drainage out of the bottom of the root zone,  $\rho_w$  the density of the water,  $\theta_s$  the saturated soil moisture content,  $C_1$  and  $C_2$  the force and restore coefficients for soil moisture, and  $\theta_{geq}$  the equilibrium surface volumetric moisture content describing the hypothetical state when gravity balances the capillary forces such that there is no vertical water flow into or out of the thin surface zone of depth  $d_1$  (Noilhan and Planton, 1989).

The drainage formulation that we adopt (unit gradient) to estimate  $q_2$  is different from that of Mahfouf and Noilhan (1996) and is described in Albertson and Kiely (2001). The value of  $\theta_{geq}$  is a function of  $\theta_2$  and the soil hydraulic properties as derived by Noilhan and Planton (1989)

$$\theta_{geq} = y \theta_s \quad (7)$$

$$y = x - ax^p (1 - x^{8p}) \quad (8)$$

$$x = \frac{\theta_2}{\theta_s} \quad (9)$$

with the two parameters  $a$  and  $p$  adjusted according to soil texture, since they account in a lumped sense for soil hydraulic properties. The relationships between soil moisture,  $\theta$ , hydraulic conductivity,  $k$ , and matrix potential,  $\psi$  are described by:

$$\psi = \psi_s \left( \frac{\theta}{\theta_s} \right)^{-b} \quad (10)$$



$$k = k_s \left( \frac{\theta}{\theta_s} \right)^{2b+3} \quad (11)$$

where  $k_s$  is the saturated hydraulic conductivity,  $\psi_s$  the air entry potential and  $b$  the slope of the retention curve in logarithmic space (Clapp and Hornberger, 1978).

The force and restore coefficients  $C_1$  and  $C_2$  are described by

$$C_1 = C_{1sat} \left( \frac{\theta_s}{\theta_g} \right)^{\frac{b}{2}+1} \quad (12)$$

$$C_2 = C_{2ref} \left( \frac{\theta_2}{\theta_s - \theta_2 + \theta_l} \right) \quad (13)$$

where  $C_{1sat}$  and  $C_{2ref}$  are parameters capturing effects of soil texture and  $\theta_l$  is a small numerical value that constrains  $C_2$  as  $\theta_2$  approaches  $\theta_s$  (Noilhan and Planton 1989). The  $C_{1sat}$  and  $C_{2ref}$  values are estimated from the literature on the basis of soil texture (Noilhan and Planton 1989).

The model needs the following meteorological data as input:

Atmospheric temperature,  $T_a$ , [K], Relative humidity,  $rh$ , [%], Rainfall,  $P$ , [mm], Atmospheric pressure,  $p_a$ , [Hpa], Wind velocity,  $va$ , [ $m\ s^{-1}$ ], Shortwave radiation,  $R_{swin}$ , [ $W\ m^{-2}$ ].

Model parameters are given in the following table (Table 2).

Table 2. Hydrological model parameters

Symbol	Unit	Description	Local value	Basin average	Std. dev
$\theta_{sat}$	$-m^3m^{-3}$	Soil moisture at saturation	0.52	0.44	0.07
$\theta_{wilt}$	$-m^3m^{-3}$	Wilting point	0.05	0.16	0.06
$\theta_{lim}$	$-m^3m^{-3}$	Field capacity	0.2	0.25	0.05
$K_{sat}$	$m\ s^{-1}$	Soil Hydraulic conductivity	0.0000001	0.0000004	0.0000003
$\psi_{sat}$	m	Soil potential at saturation	0.6	0.36	0.07
B	-	Slope of soil retention curve	8.5	6.63	2.37
$f_v$	%	Fraction of vegetation cover	Variable during the year		
$R_{smin}$	$s\ m^{-1}$	Minimum surface resistance	70	100	12
LAI	$-m^2m^{-2}$	Leaf area index.	Variable during the year		
$\alpha$	-	Albedo	0.2	0.14	0.039
C2Ref	-	Value of C2 for $\theta_2=\theta_{2sat}$	2.2	1.06	0.6
C1Sat	-	Value of C1 at saturation	0.00016	0.2	0.09
d2	M	Soil depth	0.32	0.65	0.35

The model outputs are the following variables whose values are in part reported for the period of intense observation (April 17 2003 - September 24 2004): Surface temperature,  $T_s$ , [K], representative of bare soil and vegetation, Average surface temperature,  $T_2$  [K], Soil water content,  $\theta_g$  [%], Soil water content in the root zone,  $\theta_2$  [%], Net radiation,  $R_n$  [ $Wm^{-2}$ ], Latent and sensible heat flux, LE and H [ $Wm^{-2}$ ]

## 5.1. Results at field scale

First we applied the model at field scale, in particular we simulated the field at the Nurri meteorological tower. Part of the output data from the force restore method are plotted against the observed ones for the simulation period (April 17 2003 - September 24 2004).

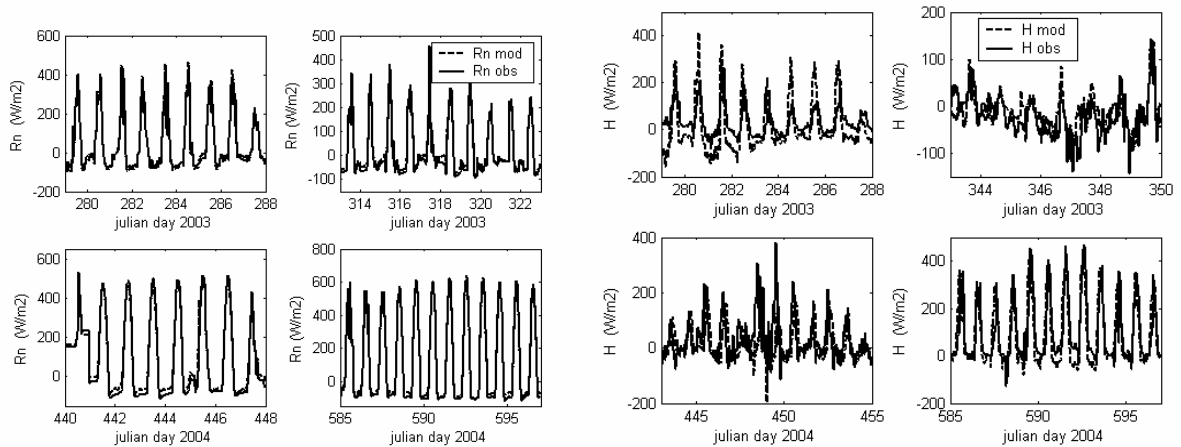


Figure 7. Net Radiation flux observed (continuous line) and modeled (dash line) on the left and sensible heat flux observed (continuous line) and modeled (dash line)

Effective evapotranspiration (Figure 8) and soil moisture computed in the two soil layers are given for the same field (Figure 9). As it is observable the computed and observed effective evapotranspiration show a good agreement in terms of fluxes and cumulative value, as well as soil moisture behavior seems also well simulated from the water budget model.

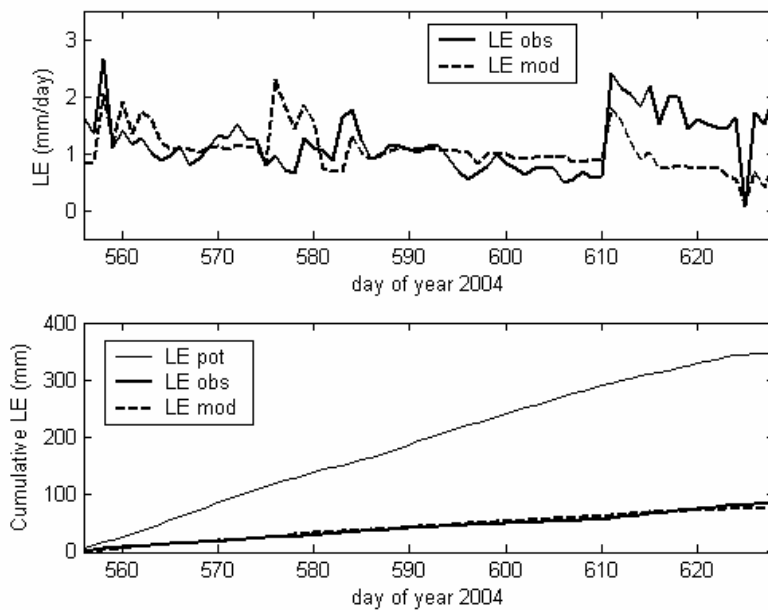


Figure 8. Daily rate and cumulative effective evapotranspiration observed (continuous line) and modeled (dash line). In the bottom figure a comparison with the potential evapotranspiration is also given.

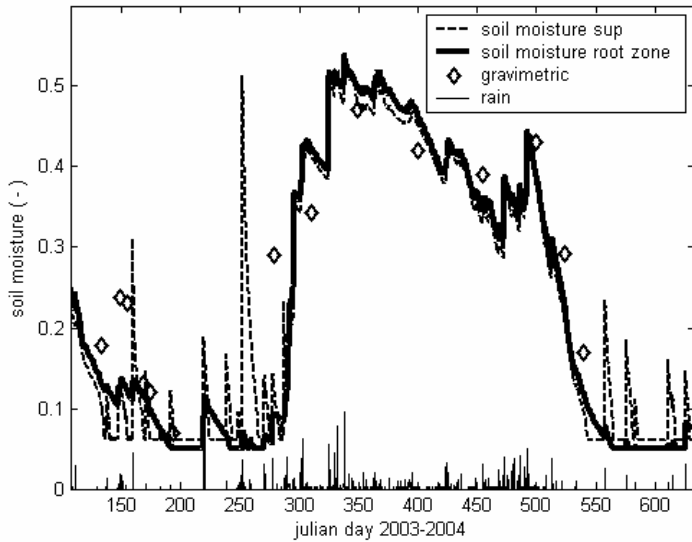


Figure 9. Soil moisture behavior at the meteorological station field. Comparison of model simulations in the shallow and deeper soil layer, ground measurement.

## 5.2. Basin scale application: comparison of soil moisture from radar and water balance model

After model validation at the station site the water balance model is applied for the whole basin using a pixel resolution of 100 m, and all the distributed information available.

Basin average soil moisture behavior is plotted for the whole observation period (Figure 10) against ground measures and retrieved soil moisture from radar data. In addition, due to the distributed scheme of the model, validation of the simulation outputs are possible for each the field (Figure 11) selected in the basin area (Figure 1).

Results from hydrological modeling, radar data and ground measures show a satisfactory simulation accuracy of this type of modeling approach and seems to be promising for the next research steps.

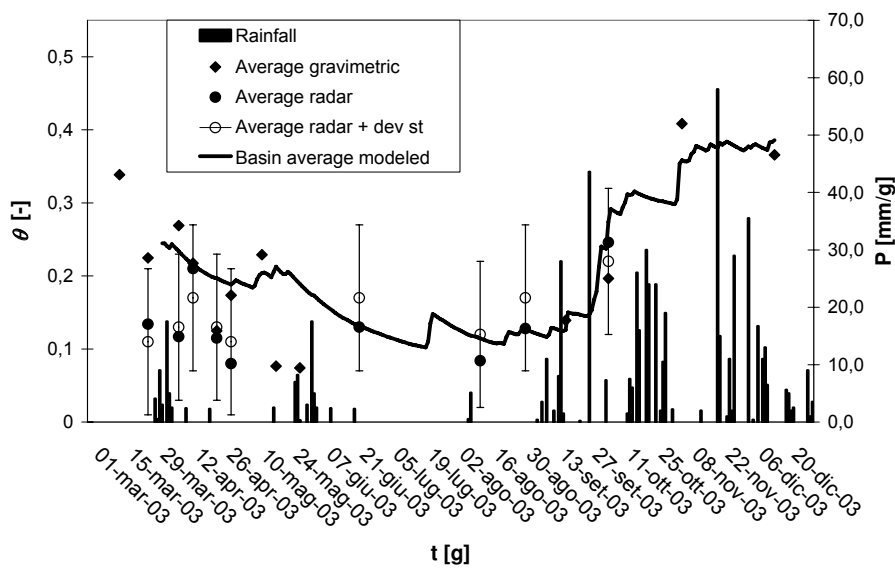


Figure 10. Time series of rainfall and ensemble-averaged soil moisture for the Mulargia basin.

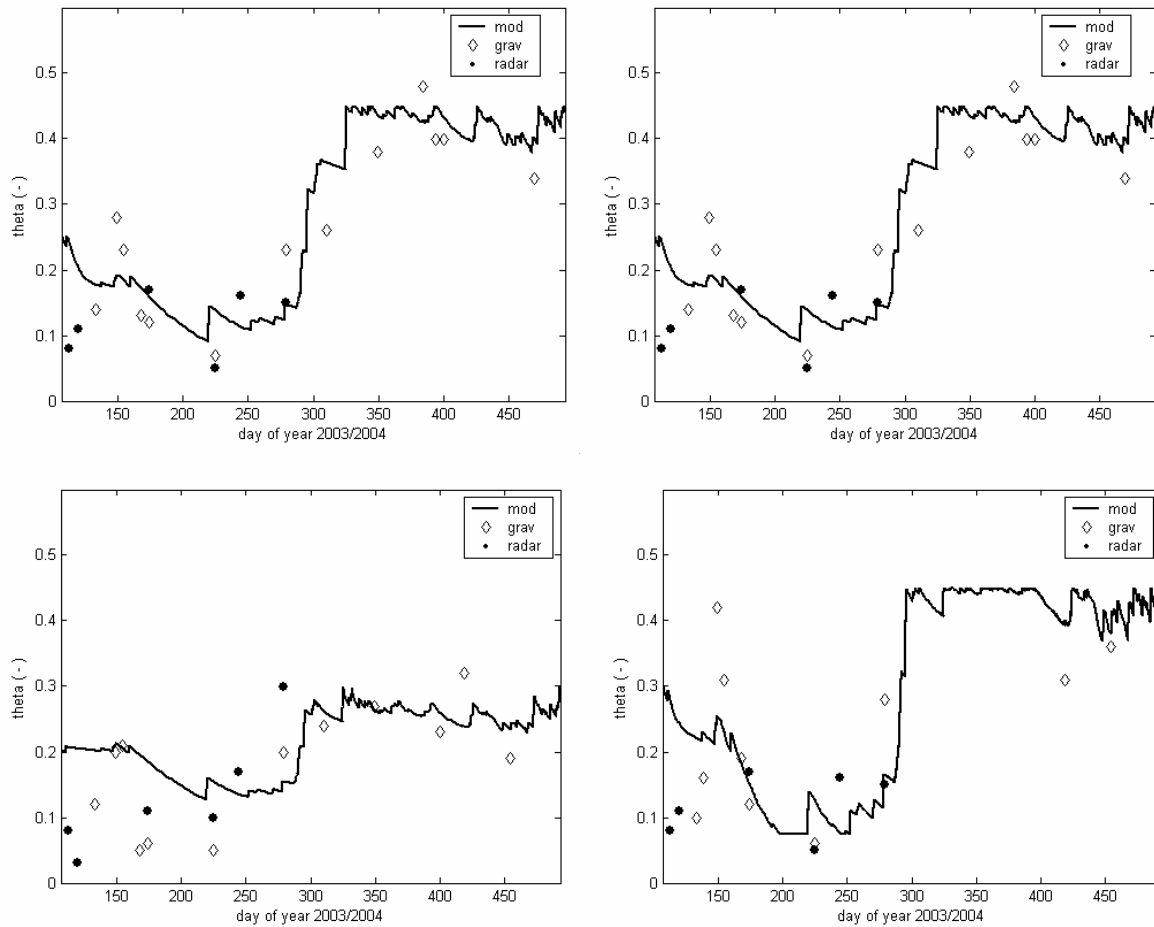


Figure 11. Field average soil moisture from modelling, ground data and radar observation for Field\_A(top left) Field\_E ( top right), Field\_F ( bottom left), Field\_G (bottom right).

## 6. CONCLUSION

The paper present an application of an energy budget model to the water balance in an Italian semiarid zone showing a possible synergism with the information retrieved from remote sensing. This is done with the aim to improve the computational accuracy of the water balance so that a more controlled irrigation practice can be performed. With this aim in the paper the vegetation LAI parameter is estimated from satellite information, while the soil moisture retrieved from radar data was used as “ internal” validation of the distributed water budget scheme.

The vegetation parameterization is performed exploring the potentiality of the Quickbird satellite images for compute the leaf area index with the aid of ground measurement and used instead than traditional crop coefficient for compute vegetation evapotranspiration. Comparison from observed and simulated value of effective evapotranspiration seems to encourage the proposed approach for irrigation districts.

Estimation of surface soil moisture from radar remote sensing show considerably good agreement with modelling result. This approach allow the model validation checking the internal state variable in addition to the classical check on the runoff volume performed at basin outlet when gauge station are available.

## Acknowledgments

The authors, which contribution to the paper is equal, thanks the Prof Vacca, Ing. P. Botti, Dr. M.A. Dessena and G. Borghero from the Water district authority Ente Autonomo Flumendosa, for the logistic and data support.

This work was supported by the Ministero dell'Università e della Ricerca Scientifica e tecnologica of Italy through grant # 2003084552\_003, and the Istituto Nazionale della montagna (Agenzia 2002).

## REFERENCES

- Brutsaert, W., 1982. Evaporation into the Atmosphere. Kluwer Academic Publ., Dordrecht, Holland, p. 299.
- Carlson, T. N., and D. A. Ripley. 1997. On the relation between NDVI, fractional vegetation cover, and leaf area index. *Remote Sensing of Environment*. (62): 241-252.
- Chen, J. M., and J. Cihlar. 1996. Retrieving leaf area index of boreal conifer forests using landsat TM images. *Remote Sensing Of Environment*. (55): 153-162.
- D'Urso G., and Santini A., 2001, Sviluppo di un sistema informativo geografico per la gestione dei comprensori irrigui, in *Modelli di agricoltura sostenibile per la pianura meridionale: gestione delle risorse idriche nelle pianure irrigue*, edito da L. Postiglione, A. Santini e M. Fagnano, Salerno, 36-44
- Famiglietti, J. S., and E. F. Wood. 1994. Multiscale modelling of spatially variable water and energy balance processes, *Water Resour. Res.*, 30, 3061-3078.
- Friedl, M. A., et al.. 1995. Scaling and uncertainty in the relationship between the NDVI and land surface biophysical variables: An analysis using a scene simulation model and data from FIFE. *Remote Sensing of Environment*. (54): 233-246.
- Fung A.K., Li Z., Chen K.S., "Backscattering from a randomly rough dielectric surface, "IEEE Trans. Geosci. Remote Sensing, vol. 30, pp. 356-369, 1992.
- Gupta, R. K., et al.. 2000. Relationship between LAI and NDVI for IRS LISS and LANDSAT TM bands. *Remote Sensing For Land Surface Characterisation*. (26): 1047-1050.
- Mancini, M., R. Hoeben, and P. A. Troch. 1999. Multifrequency radar observations of bare surface soil moisture content: A laboratory experiment, *Water Resour. Res.*, 35(6): 1827-1838.
- Montaldo N., and J. D. Albertson. 2001. On The Use Of The Force-Restore SVAT Model Formulation For Stratified Soils, *J. Hydrometeorol.*, 2(6): 571-578.
- Quesney A., Hegarat-Masclé S., Le Taconet O., Vidal-Madjar D., Wigneron P.J, (2000), Estimation of watershed soil moisture index from ERS/SAR data, *Remote Sensing Environm.* 72:290-303
- Noihlan, J., and S. Planton. 1989. A Simple parameterization of Land Surface Processes for Meteorological Models, *Mon. Wea. Rev.* (117): 536-549.
- Piervitali E, Conte M, Colacino M, Rainfall over the Central-Western Mediterranean basin in the period 1951-1995. Part II: Precipitation scenarios, *Nuovo Cimento, C* 22 (5): 649-661, 1999.
- Schmugge T., 1985, Remote Sensing of soil moisture. *Hydrological Forecasting*, edited by M.G. Anderson and T. P. Burt, John Wiley & Sons.
- Showstack, R., 2001, Desertification treaty includes key role for scientists, *EOS, Trans. AGU*, vol. 82 (27).
- Rodriguez-Iturbe I., 2000, Ecohydrology: A hydrologic perspective of climate-soil-vegetation dynamics *Water Resour. Res.*, 36 (1): 3-9.
- Topp, G., C., J.L. Davis and A.P. Annan, Electromagnetic determination of soil water content: measurements in coaxial transmission lines, *Water Resour. Res.*, 16(1): 574-588
- Welles, J. M., and J. M. Norman. 1991. Instrument For Indirect Measurement Of Canopy Architecture. *Agronomy Journal*. (83): 818-825.